THE JOURNAL OF PHYSICAL CHEMISTRY C
A JOURNAL OF THE AMERICAN CHEMICAL SOCIETY

pubs.acs.org/JPCC

Article

Fundamental Insight into Humid CO_2 Uptake in Direct Air Capture Nanocomposites Using Fluorescence and Portable NMR Relaxometry

Glory A. Russell-Parks, Noemi Leick, Maxwell A. T. Marple, Nicholas A. Strange, Brian G. Trewyn, Simon H. Pang, and Wade A. Braunecker*

Cite This: *J. Phys. Chem. C* 2023, 127, 15363−15374

Read Online

ACCESS | Metrics & More | Article Recommendations | Supporting Information

ABSTRACT: Direct air capture (DAC) technology is being explored as a pathway for reducing greenhouse gas emissions through the efficient removal of CO_2 from the atmosphere. However, there remains a knowledge gap regarding structure−property−performance factors that impact the behavior of these systems in diverse, real-world environments. In aminopolymer-based DAC systems, gas diffusion is tightly coupled with polymer mobility, which is in turn affected by a large matrix of variables, including interactions with the pore wall of the support, nanoconfinement, the presence of co-adsorbates (moisture), and electrostatic cross-links that develop as a function of CO_2 chemisorption. Higher-throughput, benchtop techniques for studying and understanding mobility in these systems would lead to more rapid advances in the field. Here, we demonstrate the value of a fluorescence technique for monitoring polymer mobility within nanocomposite capture materials as a function of CO_2 and water adsorption in a series of humidified polyethylenimine-Al_2O_3 composite materials. The approach allows us to correlate changes in mobility with CO_2 adsorption kinetics as a function of relative humidity. We further couple this information with NMR relaxometry data attained using a portable single-sided magnetic resonance device, and we employ diffuse reflectance infrared Fourier transform spectroscopy to correlate the formation of different relative amounts of carbamates and carbonates with the environmental conditions. These results provide a blueprint for using benchtop techniques to promote fundamental understanding in DAC systems that can in turn enable more efficient operation in real-world conditions.

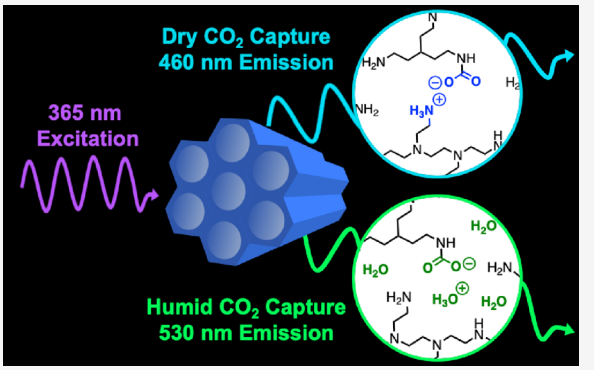

INTRODUCTION

While the global clean energy transition continues to gain momentum,[1] certain industries will be intrinsically difficult to fully decarbonize.[2] Achieving net zero carbon emissions in those instances will ultimately require the use of robust carbon capture, utilization, and storage technologies.[3] The deployment of negative emissions technology is also projected to play an increasingly important role in limiting the effects of anthropogenic climate change.[4−6] Among the direct air capture (DAC) technologies currently being investigated for pilot and commercial scale deployment, solid adsorbents based on supported amines are garnering much enthusiasm.[7] Indeed, a diverse array of recent work studying nonvolatile amino-polymers loaded onto mesoporous oxide composites is driving extraordinary advances in the field.[8−14] However, certain fundamental knowledge gaps remain that will influence how these and similar materials are employed over long cycle times,[15−17] in different environments,[18,19] and within different operational design constraints in real-world DAC systems.[20]

One such knowledge gap involves structure−property−performance relationships associated with polymer segmental mobility in confinement.[21] The mobility of these amino-polymer sorbents directly influences gas diffusion through these materials.[22] As CO_2 reacts with available amines within the polymer matrix, the formation of electrostatic cross-links in the form of carbamate species can significantly rigidify the polymer,[23] effectively converting it from a liquid or rubbery sorbent into a glassy encapsulant. The physical state of the polymer adsorbent not only affects optimal cycle times for CO_2 sorption; it also governs subsequent O_2 diffusion in and out of the material. As residual oxygen in the sorbent chamber during the CO_2 desorption step can lead to fast sorbent degradation,[24] selective O_2 removal prior to CO_2 desorption plays a key role in optimizing amine-based sorbent lifetimes. This optimization

Received: May 30, 2023
Revised: July 12, 2023
Published: July 26, 2023

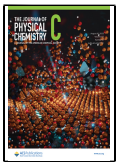

requires fundamental understanding of gas diffusion in these materials and hence polymer mobility.

Aminopolymer mobility is governed by a matrix of complex and often counterbalancing factors. These include the architecture and molecular weight of the polymeric sorbent;[25] surface and interface effects in thin films;[26−28] the presence of moisture and other additives that can serve as plasticizers[23] and even change the mechanism of adsorption;[29] partial degradation of the sorbent[30] that can lead to rigid moieties[31] in the polymer; and relative CO_2 uptake that results in various degrees of ionic cross-linking.[13] These combined effects on polymer mobility are further influenced and compounded in nano- and mesoporous confinement.[32−34] We recently outlined the merits and drawbacks of an array of techniques for studying polymer mobility in confinement,[35] which included differential scanning calorimetry,[36] dielectric spectroscopy,[37] NMR,[21] and neutron scattering,[38,39] among others.[40,41] However, given the large matrix of variables that influence polymer mobility in confinement that can change as a function of lifetime and cycling, higher-throughput techniques for quantifying mobility could lead to more rapid advances in the understanding and deployment of these materials in DAC systems.

Various fluorescent probes have been employed to study polymer mobility and have proven particularly useful for studying mobility in thin films and in confinement where other techniques encounter limitations.[42−45] We recently detailed the development of a powerful fluorescent probe designed specifically to study aminopolymer mobility, and we demonstrated its usefulness in studying DAC sorbents.[35] Here, we build on that foundational study by examining polyethylenimine (PEI) mobility as a function of CO_2 uptake across a wide range of temperatures and relative humidity (RH) in a mesoporous γ-Al_2O_3 composite. We further couple this information with NMR relaxometry data attained using a versatile and portable magnetic resonance device known as NMR Mobile Universal Surface Explorer (MOUSE).[46] We then employ diffuse reflectance infrared Fourier transform spectroscopy (DRIFTS) to correlate the formation of different relative amounts of carbamates and carbonates with the environmental conditions. This approach provides a blueprint for using benchtop analytical techniques to promote fundamental understanding of structure−property−performance relationships that can in turn enable more efficient operation of DAC materials in a variety of real-world climates and environments.

METHODS

Materials. Tetrakis(4-hydroxyphenyl)ethylene (THPE) was purchased from TCI. Branched polyethylenimine (PEI; M_n = 600 g/mol, M_w = 800 g/mol) was purchased from Sigma; prior to use, PEI was stirred and heated at 100 °C under 25 mTorr vacuum for 72 h to remove any residual volatile organics. Mesoporous γ-Al_2O_3 was purchased from Sasol and dried at 100 °C under 25 mTorr vacuum overnight prior to any use. All other reagents and chemicals were purchased from Aldrich and used without purification, unless otherwise noted.

Composite Preparation. Sorbents were prepared by first doping bulk PEI (1 g) with 1 wt % THPE (10 mg) and stirring under N_2 in the dark at 50 °C for 1 h. Mesoporous γ-Al_2O_3 (1.5 g) was then impregnated with this mixture, targeting a ∼70% pore fill, by first stirring doped PEI and Al_2O_3 in separate methanol solutions (∼10 mg/mL) for 1 h, and then combining and stirring overnight. Methanol was removed from this combined mixture with a rotary evaporator. The composite was then dried at 25 mTorr vacuum overnight at 100 °C in the dark. Thermogravimetric analysis (TGA) was employed to verify that the weight fraction of PEI in the composite was ∼40 wt %.

Relative Humidity. Samples were pre-equilibrated to a given RH with the following procedure: 150 mg of 40 wt % PEI:Al_2O_3 was evenly dispersed into five quartz cuvettes (30 mg in each). Five different aqueous saturated salt solutions were prepared to create chambers with five different RH values. Nitrogen was bubbled through each saturated solution overnight to remove oxygen. Using an N_2-purged glovebag, the cuvettes were transferred under N_2 into the chambers, which were then sealed. The samples equilibrated at a given RH for 72 h before the chambers were opened and the cuvettes were quickly sealed with a Teflon-lined cap. The PEI:Al_2O_3 composites were weighed before and after the 72 h equilibration time to calculate the mass of water adsorbed. For experiments that required both flowing gas and the maintenance of a given RH, a set of mass flow controllers was employed. Dry 400 ppm CO_2 in N_2 passed through one controller, and a second stream of 400 ppm CO_2 in N_2 passed through a separate controller and then a water bubbler. These lines were then combined into one stream for tuning RH, passed through a given sample, and then connected as exhaust gas to a LiCOR 850 quantitative CO_2/H_2O analyzer.

TGA. PEI content in the Al_2O_3 composite was estimated using a TA Instruments Q600 TGA apparatus according to a literature procedure.[47] Weight loss from 120 to 900 °C under a 100 mL/min flow of N_2 diluted air was recorded at 10 °C/min and normalized by the residual mass at 900 °C.

Photoluminescence (PL) Spectroscopy. PL experiments were performed on a custom-built Princeton Instruments spectrometer using a liquid N_2-cooled Si CCD (PyLoN) array for collecting the visible−NIR spectra (400−900 nm). Intensity calibration was preformed daily using an IntelliCal USB-LSVN (9000-410) calibration lamp. Samples were placed in a 2 mm quartz cuvette and excited with a 365 nm LED (7.5 nm FWHM) in an oxygen-free environment. A 400 nm longpass filter was employed between the sample and the collection fiber. The emission spectra were collected from 200 to 800 nm using a 150 g/mm grating with an 800 nm blaze and a 3 mm slit; 20 spectra were averaged with an overall exposure time of ∼5 s for each measurement. Temperature control was achieved with an Oxford Instruments OptistatDN sample-in-N_2-vapor cryostat. Unless otherwise specified, polymer samples were both cooled and heated at a rate of ∼1 °C/min. The standard error was calculated by dividing the standard deviation by the square root of the sample size, typically attained from three different independent samples.

MOUSE T_1 and T_2 Relaxometry Measurements. T_1 and T_2 NMR relaxometry measurements were carried out with a single-sided PM2 NMR MOUSE from Magritek GmbH, operating at a frequency of 28.05 MHz for ^{1}H with a static magnetic field gradient of 39.9 T/m. Signals are detected by a horizontal slice detection area of 12.5 × 12.5 mm^2 configured to a max penetration depth of 1.9 mm. For these measurements, a slice thickness of ∼50 μm (acquisition time of 12 μs) was used to reduce the echo time and maximize the acquisition volume of the signal.

https://doi.org/10.1021/acs.jpcc.3c03653
J. Phys. Chem. C 2023, 127, 15363−15374

As these samples were contained within a small vial as loose powder, at the start of each measurement, a rapid profile incrementing 50 μm steps over the full depth range was first taken to observe the location of the maximum signal and the position of the stage was then moved to that location for the T_2 and T_1 measurements. A radio frequency pulse length of 1.8 μs with varying amplitudes was used for the 90 and 180° pulses in the CPMG and T_1 saturation recovery experiments for measuring T_2 and T_1, respectively. For the CPMG experiments, an echo time of 32 μs was used with 1000 echoes totaling 32 ms in acquisition time, and between 64 and 512 scans were acquired to improve the signal to noise. For T_1 saturation recovery experiments, the recovery delay was incremented exponentially with 24 steps between 0 and 1200 ms max recovery time, and a CPMG detection was used for detecting each T_1 recovery increment using the same echo time of 24 μs, co-adding the first 10 echoes, and acquiring 64 scans to improve the signal to noise. The error bars on T_2 values in Figure 4 represent the standard deviation error calculated from the covariance output of the scipy.optimize.curve_fit function in Python that uses a nonlinear least-squares analysis.

DRIFTS. The surface intermediates formed during the PEI:Al_2O_3 and CO_2 interactions with varying levels of RH were monitored with DRIFTS. A praying mantis cell from Harrick Scientific was employed with ZnSe windows that remains optically transparent between 4000 and 800 cm^{-1}. The samples were pre-humidified for 72 h prior to any measurements and were then transferred to the DRIFTS cell. Upon closing the cell, a background was immediately collected over 256 scans and with a 4 cm^{-1} resolution. Subsequently, 100 sccm of anhydrous or humid CO_2 stream was introduced into the chamber, and the difference spectra were recorded after 5, 10, 15, 20, 25, 30, 60, and 90 min after the background was acquired. Because of the gas flow, a loss of some of the powder with time from the sample holder attenuated the signal intensity over 90 min from ∼5 to 4. After each sample, the humidity of the CO_2 stream was adjusted and equilibrated using a LiCOR 850 in line with the exhaust line, which was also used to monitor the CO_2 and H_2O concentrations in the gas stream.

RESULTS AND DISCUSSION

Moisture and Fluorescence. We previously detailed the merits of employing fluorescent probes based on tetraphenylethylene (TPE) in a proof-of-concept study for qualitatively comparing aminopolymer mobility across confined mesoporous DAC composites.[35] Here, we develop these probes further to study branched PEI mobility in model DAC systems as a function of real-world operating conditions, beginning with moisture uptake as a function of RH exposure. PEI composites with γ-Al_2O_3 are quite hygroscopic;[24] a composite that is 40 wt % PEI can uptake as much 1.7 equivalents in weight of water relative to PEI when allowed to equilibrate in a stream of humid N_2 (*vide infra*). This amount of moisture can significantly alter the mobility of the PEI matrix. However, disentangling the effects of moisture on the fluorescence response of these probes requires a thorough understanding of the quenching mechanisms at play.

TPE-based molecules behave as aggregation-induced emission (AIE) probes; they tend to be non-emissive when well solvated in low or non-viscous solvents, where unrestricted intramolecular rotations provide non-radiative pathways for excited state decay. However, when these rotations become restricted to varying degrees, a strong wavelength-dependent emission is observed from TPE that is a function of the mobility of its matrix. More details of the mechanism responsible for this behavior have been thoroughly reviewed elsewhere.[48,49] In short, the temperature-dependent emission of TPE has been explained primarily on the basis of two emissive states. Emission from the Franck−Condon state, corresponding to the minimal change in the nuclear coordinates of the molecule, occurs near 460 nm and is observed when TPE is either contained within frozen/glassy media or is highly aggregated. When dispersed in viscous liquid media, conformational relaxation of TPE to a planar state can occur as the molecule rotates around the excited (π−π*) state ethylenic bond, leading to emission near 530 nm. We note that while the excited state kinetic behavior of TPE has been well documented in these different media for more than 40 years, the nuclear dynamics immediately following photoexcitation in TPE and its derivatives continue to be studied and debated.[50,51]

In contrast to aggregation-caused quenching probes such as perylene,[52] where water can induce aggregation and π-stacking interactions that open non-radiative decay pathways, the addition of water to a non-emissive AIE probe solution will often induce aggregation and turn on fluorescence. While high energy vibrations in water molecules can themselves quench fluorescence,[53] the restriction of intramolecular rotation appears to dominate the fluorescence response of most AIE probes in aqueous solutions.

In this work, we employ tetrakis(4-hydroxyphenyl)ethylene (THPE) as our probe. The hydroxyl groups dramatically enhance its solubility in PEI relative to the parent TPE compound. Correll et al. recently demonstrated that THPE emits near 460 nm and appears blue in a frozen/glassy/aggregated state, while it appears green and emits closer to 530 nm in a viscous PEI solution.[35] While TPE derivatives are much more commonly employed as AIE rather than ratiometric probes, that initial work demonstrated how a ratiometric analysis of the emission of THPE could be used to accurately assess aminopolymer and small-molecule melting points and glass transitions. The efficacy of the probe was benchmarked in 12 systems with melting points spanning ∼200 °C, both in the bulk and in confined mesoporous oxides. Ratiometric analysis was used to assess additional physical phenomena in that work, including polymer hysteresis. In a second study, Li et al. demonstrated that a similar ratiometric analysis of THPE emission could serve as a measure of the relative mobility of several different epoxide-functionalized aminopolymers with different degrees of hydrogen bonding.[54] Fluorescence data was correlated with NMR relaxometry data to provide more quantitative analysis of polymer mobility.

Here, we begin assessing the fluorescence response of THPE under DAC operating conditions, starting with the effects of moisture. We first prepared a series of THPE solutions in PEI and water to determine the relative volume fractions at which we could attribute emission changes to changes in polymer mobility and at what volume fractions of water AIE begins to dominate. The fluorescence of THPE in mixed alcohol/water solutions was recently investigated.[55] Between 0 and 82 vol % water in ethanol, no THPE fluorescence could be detected as the probe was still well solvated. Only when the water fraction was at or above 84 vol % was blue emission observed, as THPE began to aggregate. In our aqueous PEI solutions, where the

https://doi.org/10.1021/acs.jpcc.3c03653
J. Phys. Chem. C 2023, 127, 15363−15374

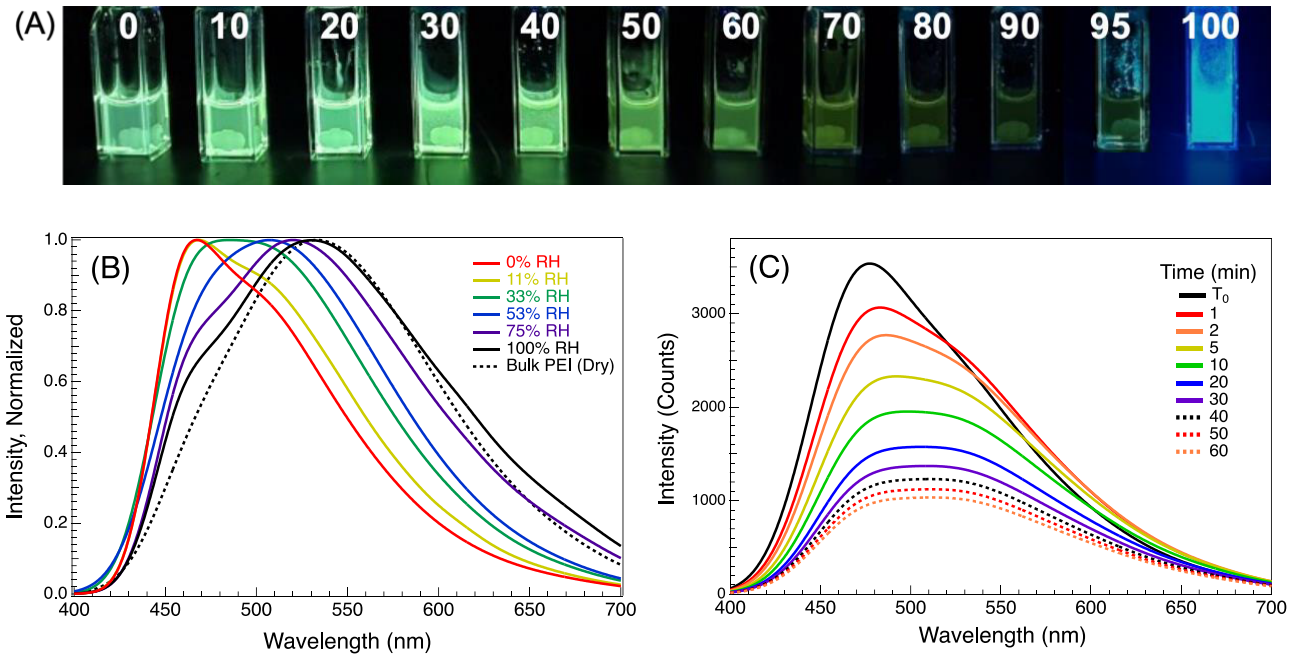

Figure 1. (a) Series of aqueous PEI solutions (0−100 vol % water) containing 0.1 wt % THPE irradiated at 365 nm. The intensity of the green fluorescence systematically decreases as the aqueous PEI solutions become less viscous until above 90 vol % water, when THPE begins to aggregate and emit blue light. (b) Fluorescence spectra of 0.4 wt % THPE in a 40 wt % PEI:Al_2O_3 composite after equilibrating to a given RH for 72 h. (c) Change in the fluorescence of a dry composite of 0.4 wt % THPE in 40 wt % PEI:Al_2O_3 as a function of time upon exposure to 100 sccm of a humidified stream of N_2 (100% RH). Measurements performed at 25 °C.

concentration of the probe was 0.1 wt % relative to the total mass of the solution, we only observed green fluorescence between 0 and 90 vol % water. As can be seen in Figure 1a, the intensity of the fluorescence systematically decreases as the water content increases and sample viscosity decreases. However, between 90 and 95 vol % water, THPE began to aggregate and stick to the walls of the cuvette, where its blue emission could be observed. Bright blue emission was pronounced in 100% water, where THPE formed a heterogeneous suspension. The results suggest that changes in the photoluminescence quantum yield (PLQY) of THPE as a function of water concentration in aqueous PEI solutions ≤90 vol % water are not caused by probe aggregation. We acknowledge that the results in bulk solutions are not perfectly transferable to confined systems. Even though the overall fraction of water present in composites equilibrated at 100% RH (*vide infra*) is considerably lower than what we measured here in the bulk, it is known that confinement can, in some cases, change the solubility of small molecules relative to bulk solutions.[56] However, the results are an important first step in quantifying the AIE response of THPE in humidified PEI.

Turning to confined systems, we then prepared a series of composite samples equilibrated for 72 h at different values of RH according to a procedure described in the Methods section. The amount of water adsorbed by a 40 wt % PEI composite (12 mg of PEI in 18 mg of Al_2O_3) at each RH is recorded in Table 1. A systematic increase in moisture uptake between ∼2 and 20 mg is observed in this series. The composite also contained ∼0.4 wt % THPE. The emission spectrum of each humidified composite is illustrated in Figure 1b. The emission λ_{max} are recorded in Table 1.

Several observations are worth noting about the data in Figure 1b. First, if we compare the dry bulk PEI spectrum with that of the dry composite, there is a dramatic blueshift in the

Table 1. Moisture Uptake in PEI:Al_2O_3 Composites and Corresponding Influence on Fluorescence[a]

sat. salt solution	RH (%)	H_2O uptake (mg)	emission λ_{max} (nm)[b]
	0		468
LiCl	11	1.8	469
$MgCl_2$	33	4.0	486
$Mg(NO_3)_2$	53	6.2	508
NaCl	75	10.4	520
distilled H_2O	100	20.2	530

[a]30.0 mg of a 40 wt % PEI:Al_2O_3 composite (12.0 mg of PEI and 18.0 mg of Al_2O_3) was equilibrated for 72 h in a sealed chamber with a given saturated salt solution. [b]0.4 wt % THPE present in the composite was excited at 365 nm.

emission from λ_{max} of 533 nm to near 468 nm in confinement, consistent with a sharp reduction in the mobility of the polymer matrix. These results are also consistent with our previous work in mesoporous silica composites using both tethered and dispersed TPE derivatives.[35] If we then consider the samples equilibrated to different values of RH, we observe a systematic redshift in λ_{max} as a function of increasing RH. This result is consistent with the literature, which has hypothesized that moisture acts as a plasticizer for PEI chains that can weaken the inter- and intramolecular hydrogen bonding and dipole−dipole interactions in PEI,[23] all of which will enhance its mobility. Interestingly, the λ_{max} of the emission spectrum of the composite sample equilibrated to 100% RH is nearly identical to that of the bulk dry sample. A ratiometric analysis of the data at 460 and 530 nm for these particular samples suggests that the effects of confinement and humidity on mobility may effectively counterbalance each other. While care should be exercised in not overinterpreting the fluorescence response, since (as mentioned) the high energy vibrations in water molecules can themselves also contribute to

https://doi.org/10.1021/acs.jpcc.3c03653
J. Phys. Chem. C 2023, 127, 15363−15374

fluorescence quenching, the implications of these fluorescence measurements on PEI mobility are fully consistent with the NMR relaxometry data that will be presented in a subsequent section.

Finally, we monitored the fluorescence response of a dry composite by flowing 100 sccm of 100% RH N_2 through the sample over the course of 1 h (Figure 1c). The emission λ_{max} immediately begins red shifting and a new peak grows in near 530 nm, suggesting that mobility increases as the sample is becoming humidified. However, the results also indicate that the composite has not yet reached equilibrium after just 1 h. Going forward, all samples were allowed to equilibrate at a given RH for 72 h prior to further measurements or manipulation.

CO_2 Adsorption and Aminopolymer Mobility. Two samples of a 40 wt % PEI:Al_2O_3 composite (0.4 wt % THPE) were prepared. The first was kept under a dry, inert (N_2) environment, and the second was saturated with CO_2 in a stream of simulated flue gas (45 sccm of N_2 and 5 sccm of CO_2) for 12 h at 30 °C. The fluorescence spectrum of each sample was then recorded at 30, 0, and −30 °C. In previous work,[35] we demonstrated how quantifying the emission spectra *via* ratiometric analysis at two wavelengths as a function of temperature can give accurate indication of relative polymer mobilities across different samples. Here, we perform this analysis at these three temperatures as we flow CO_2 over the pristine composite. We then compare how much the mobility of the polymer changes at a given temperature relative to its theoretical "limit" when saturated with CO_2. The normalized data is illustrated in Figure 2.

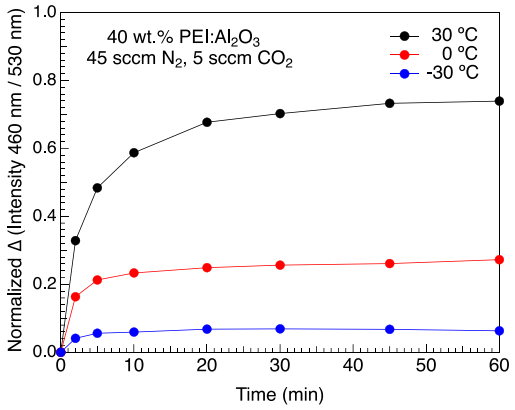

Figure 2. Normalized change in the emission spectra with time of a 40 wt % PEI:Al_2O_3 composite doped with 0.4 wt % THPE while flowing 45 sccm of N_2 and 5 sccm of CO_2 at 30 °C (black), 0 °C (red), and −30 °C (blue).

If we first consider the data at 30 °C, we observe that 75% of the total mobility change occurs within the first hour of simulated flue gas exposure (black trace, Figure 2). The remaining changes occur very slowly over the next 11 h. In contrast, after 1 h at 0 °C, mobility only changes by 30% of its theoretical limit (the limit being estimated from the amount of adsorbed CO_2 during the 12 h simulated flue gas experiment at 30 °C). Less than 10% change in mobility is seen at −30 °C in this time. The samples at 0 and −30 °C effectively level off after 1 h and do not approach their theoretical limit, even after 12 h of CO_2 exposure. The results can be rationalized by considering that PEI becomes glassier much faster or with less overall CO_2 uptake at colder temperatures, which in turn inhibits further gas diffusion and uptake. The activation barrier for CO_2 adsorption and/or proton transfer may also play a more significant role at these lower temperatures. We contend that this technique will be particularly useful for studying an array of materials and additives for understanding and optimizing sub-ambient capture processes.[18,19] We turn now to studying changes in polymer mobility under a variety of simulated DAC conditions, namely, 100 sccm of 400 ppm CO_2 in N_2 at different RH.

After equilibrating for 72 h at a given RH, a 40 wt % PEI:Al_2O_3 composite was loaded into a flow-through quartz cuvette, where the exhaust gas was routed through a LiCOR 850 quantitative CO_2/H_2O infrared analyzer. This allowed us to simultaneously monitor CO_2 sorption, RH of the sweep gas, and any changes in the emission spectra of the sample. Six different samples were equilibrated to the same RH values employed in Table 1. Changes in the emission spectra of a representative sample (at 53% RH) as a function of time and CO_2 uptake are illustrated in Figure 3a, with the emission spectra of the other samples shown in Figure S1 in the Supporting Information (SI). Changes in all six samples are quantified in Figure 3b, plotted as ratiometric intensities recorded as a function of time.

As can be seen in Figure 3a for the data at 53% RH, flowing humid CO_2 causes a blueshift in the emission spectra and an overall increase in the PLQY. The data is consistent with a decrease in polymer mobility with CO_2 uptake, and it stands in contrast to the data in Figure 1c, where flowing CO_2-free moisture over an otherwise dry system causes a redshift in the emission spectra, a decrease in the PLQY, and an increased polymer mobility. We note that while the emission band at 460 nm clearly increases as a function of CO_2 adsorption in Figure 3a, emission at 530 nm appears to first increase before then decreasing. Similar anomalies are observed in some of the data sets in Figure S1, such as a slow overall decrease in the absolute intensity of the spectra associated with 0% RH. However, since flowing gas causes the powder composite to occasionally shift in the sample holder with time, absolute fluorescence intensities of any given spectra are not all that meaningful as compared to ratiometric analysis.

When comparing the change in the ratiometric intensity of all six composites in Figure 3b, a few initial observations are worth noting. First, the drier the sample, the more rapid the polymer mobility changes and becomes glassier as it begins uptaking CO_2. Also noteworthy, the data suggests that samples between 0 and 33% RH all reach approximately the same mobility after 90 min under these conditions. Above 33% RH, mobility after 90 min of CO_2 capture trends higher with increased RH.

While polymer mobility data inferred by these fluorescence measurements is fully consistent with the NMR relaxometry data (*vide infra*), a truly quantitative assessment of mobility with this technique would require a more in-depth understanding of how nuclear motions in the probe molecule and associated emission bands are influenced by factors such as ionic strength of the media, which will change as a function of moisture and CO_2 uptake. As the impact of ionic strength on the emission spectra is not well understood for these probe molecules, here, we make only qualitative comparisons of mobility inferred by fluorescence. We did, however, perform an analysis of all the data in Figure 3b using additional sets of wavelengths, namely, 450/560 and 490/540 nm (Figure S2).

https://doi.org/10.1021/acs.jpcc.3c03653
J. Phys. Chem. C 2023, 127, 15363−15374

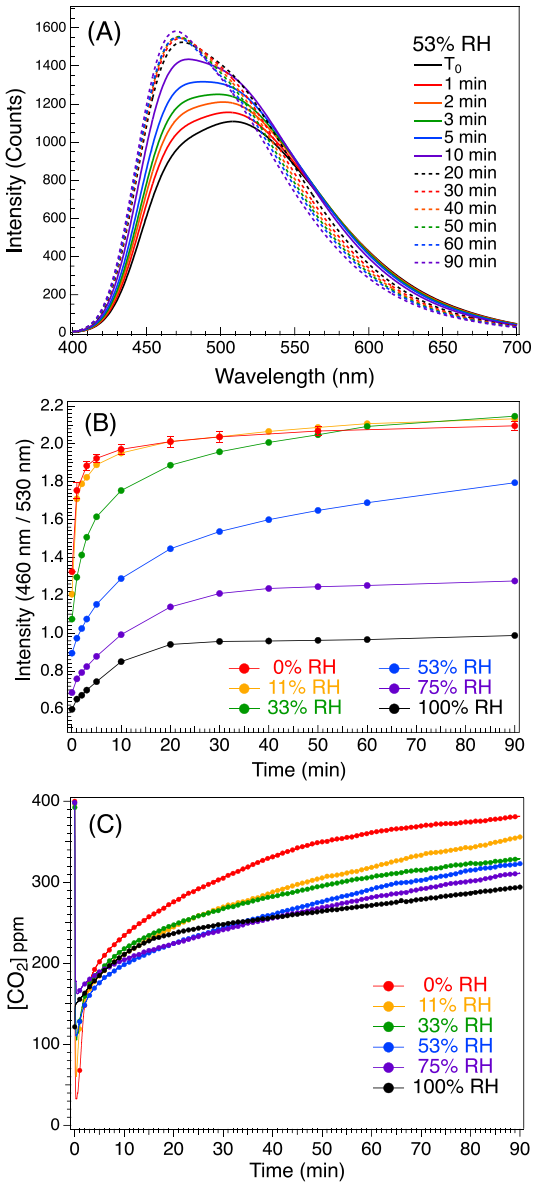

Figure 3. 40 wt % PEI:Al_2O_3 composite, 0.4 wt % THPE, pre-equilibrated to a given RH for 72 h, 100 sccm of 400 ppm humid CO_2 in N_2. (a) Change in the emission spectra with time at 53% RH. (b) Summary of ratiometric fluorescence intensity (460/530 nm) of six samples at different RH as a function of time with CO_2 flow. (c) CO_2 adsorption kinetics of a 40 wt % PEI:Al_2O_3 composite in a stream of 400 ppm CO_2 (100 sccm) at various RH.

Comparison of these data sets with that in Figure 3b (460/530 nm) reveals remarkably similar trends. None of the conclusions drawn change in any way regardless of which of these sets of wavelengths are employed for the ratiometric analysis.

A more thorough interpretation of the data in Figure 3b requires that CO_2 sorption data for these six samples be considered. We illustrate in Figure S3 of the Supporting Information how we can monitor both adsorption and desorption in a continuous stream of 400 ppm CO_2. Integration of the area between the curve and the 400 ppm baseline can be used to quantify CO_2 uptake in these experiments, with the adsorption and desorption cycles in full agreement. In Figure 3c, we plot the CO_2 adsorption data for all six samples collected concurrently with the fluorescence measurements above. When individual data traces in this figure approach 400 ppm, it is an indication that they have stopped uptaking significant amounts of CO_2 from the 400 ppm stream. A closer inspection of the data reveals that at 90 min, the driest sample is near saturation, while the sample under 100% RH has uptaken twice as much CO_2 and is still adsorbing it. Indeed, there is a strong correlation of CO_2 uptake with RH. When we consider both fluorescence and CO_2 sorption data, we observe that the dry samples become glassier much faster, despite having uptaken the same or less CO_2 than the wet samples. The results are fully consistent with the literature, where more humid conditions at low CO_2 concentrations have been mainly reported to promote CO_2 diffusion and to double the CO_2 capacity compared to anhydrous conditions.[57−61] We and others hypothesize that the relative formation of bicarbonates and certain carbamate species in the presence of moisture are responsible for different degrees of electrostatic cross-linking in these samples that in turn impact polymer mobility. We probe this hypothesis further in the next two sections by correlating the polymer mobility data inferred by fluorescence with NMR relaxometry data on these same samples. We further study the formation of different species in these reactions using DRIFTS to disentangle specific molecular contributions to polymer mobility.

NMR MOUSE. The NMR MOUSE was originally developed as a compact and mobile tool for noninvasive clinical diagnostics and the investigation of materials properties of arbitrarily large objects.[46] The technique has since been used extensively for nondestructive and in-field evaluation of rubber and elastomers, cultural heritage items, and food products.[62] Unlike traditional NMR, chemical shift information cannot be attained with this technique; however, through the detection of differences in the relaxation times of hydrogen protons, NMR MOUSE data can be used, for example, to differentiate clay-bound water vs movable water, gas, light oil, and viscous oils present in porous media.[63] Here, we use the technique to evaluate the mobility of PEI in Al_2O_3 as a function of moisture and CO_2 uptake, both to corroborate the fluorescence mobility data and also to demonstrate the value of the technique as a stand-alone diagnostic *in operando* tool for evaluating the health and performance of DAC composites in the field.

We selected 12 samples for this study, namely, the six composites listed in Table 1 that were equilibrated to different values of RH, and a set of six additional composites equilibrated to those same values of RH but exposed for 90 min to a stream of 400 ppm CO_2. The mobilities of these 12 samples were measured with fluorescence (see the first and last data points of each trace in Figure 3b). Here, we record and discuss both the transverse, spin−spin relaxation time (T_2) as well as the longitudinal, spin−lattice relaxation time (T_1) for each sample.

T_2 relaxation is a complex phenomenon influenced by a number of mechanisms, a major one being dipolar coupling between spins.[64] T_2 values for these 12 samples were determined by collecting an echo train and fitting the amplitude decay curve (Figures S4 and S5 in the SI). Ultimately, this relaxation parameter is a measure of the coherence time of the spins. Strong dipolar coupling in rigid samples induces faster decoherence, while in samples with high molecular mobility, T_2 can be longer as the process is less efficient. In polymeric systems, greater entanglements and/or cross-linking density results in a decrease in mobility that

https://doi.org/10.1021/acs.jpcc.3c03653
J. Phys. Chem. C 2023, 127, 15363−15374

manifests as shorter T_2 values.[65,66] In Figure 4, we illustrate the T_2 values collected for these 12 samples as a function of RH and CO_2 exposure.

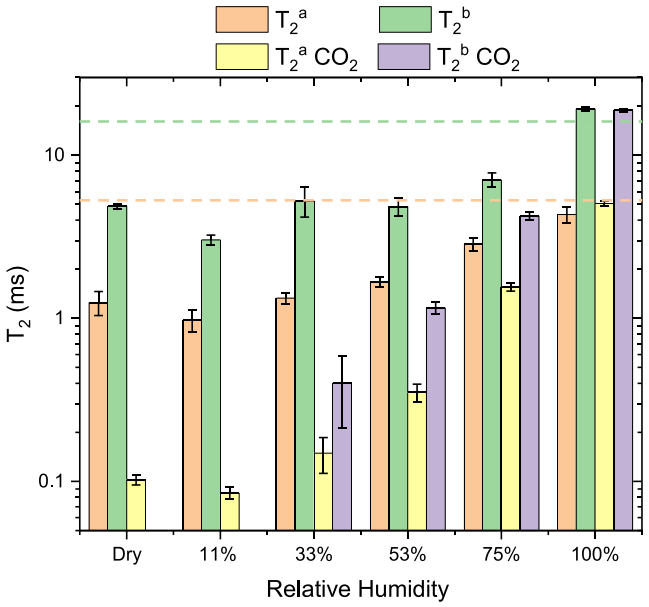

Figure 4. Transverse, spin−spin relaxation values (T_2) for 40 wt % PEI:Al_2O_3 composites, equilibrated to six different values of RH, before and after exposure to 90 min of 400 ppm CO_2 flow (T_2 and T_2 CO_2, respectively). In most samples, a biexponential fit of the echo train attenuation data was required, resulting in two components (a and b) with two distinct values of T_2. The dashed orange and green lines correspond with the a and b components, respectively, of the bulk anhydrous PEI value of T_2.

Performing an inverse Laplace transform on the T_2 echo train decay curves produces the relaxation spectra (plotted in Figures S4 and S5), showing that most spectra are bimodal with two distinct T_2 values per sample, referred to here as the "a" and "b" components of the spectrum. Thus, a biexponential function was used to constrain the fitting of the T_2 echo train decay curve to facilitate comparison between samples. This bimodality is observed even in the dry composite that has not seen CO_2 and is possibly explained by protons near the branched PEI chain ends relaxing at a significantly different rate than protons in or near the backbone, a phenomenon not uncommon for side-chain-bearing polymers.[67,68] A few general trends are worth noting from the data in Figure 4. First, for both the pristine set of samples and the set exposed to CO_2, T_2 increases with increasing RH, suggesting that moisture increases the polymer mobility. Second, PEI composites that have been exposed to CO_2 generally display shorter T_2 values than the pristine composites. This trend is particularly evident in the drier samples, indicating that CO_2 exposure results in a much more rigid matrix in drier conditions. As the RH increases, the difference in T_2 between pristine and CO_2 exposed samples begins to converge until there is no statistical difference at 100% RH. Finally, we note that T_2 measured for bulk anhydrous PEI (dashed lines in Figure 4) is quite similar to that of the PEI:Al_2O_3 composite at 100% RH. Those results are fully consistent with the mobility data implied by fluorescence (compare solid and dashed black traces in Figure 1b).

T_1 relaxation is a measure of the rate of energy transfer from the nuclear spin system to neighboring lattice molecules. The frequency of this measurement is dictated by temperature and the magnetic field strength. T_1 relaxation is also affected by dipolar spin coupling, as well as mobility of the lattice molecules, quadrupolar coupling, anisotropy, paramagnetic effects, spin diffusion, etc.[64] Overall, T_1 relaxation is a longer process than that of T_2. Because processes like polymeric mobility can serve as an energy sink from spins to the lattice, higher mobility in the lattice will lead to shorter T_1 relaxation times (in contrast to T_2). In Figure S6, we plot T_1 values for all 12 samples. Similar trends and conclusions can be inferred here regarding polymer mobility as can be inferred from the T_2 and fluorescence experiments, at least for the samples ≤75% RH. The 100% RH samples are clear outliers, being much higher in magnitude than all the other T_1 values. We believe that this phenomenon is likely due to the phase separation of large amounts of water in the 100% RH samples, which could give rise to an altogether different T_1 signal, and was recently invoked to explain other observations in humidified PEI composites.[24] That hypothesis is further supported by the DRIFTS measurements in the next section, which illustrate a dramatic increase in the stretching frequency associated with hydroxyl groups near 3650 cm^{-1} for the 100% RH sample. Regardless, the T_1 and T_2 data as a whole serve to corroborate the fluorescence mobility data and the interpretation of structure−property−performance relationships.

DRIFTS Study of Product Formation. In dry conditions, CO_2 reacts with two amines (primary or secondary) to form ammonium carbamate ion pairs (RNH_3^+ COO^-/$R_2NH_2^+$ COO^-). The stabilization of these ions over two amines not only keeps the capacity low at 0.5 mol bound CO_2 per mole of amine[59,69,70] but also contributes to cross-linking within the polymer or between polymer chains that significantly impedes subsequent CO_2 diffusion.[38,71,72] However, unlike in dry conditions, the exact molecular interactions in humid conditions are still debated. Properties such as adsorbent loading, polymer molecular weight, amine functionality, the support, its porosity, and acidity, as well as the RH and CO_2 concentration all have been reported to affect the interaction of PEI with H_2O and CO_2.[57−61] Despite all these variables, humid conditions at low CO_2 concentrations have been mainly claimed to promote CO_2 diffusion and can even double the CO_2 capacity relative to the anhydrous state.[57−61] While the general proposed mechanism in anhydrous conditions involves ammonium carbamate ion formation and cross-linking, when moisture is present, water-stabilized ammonium bicarbonate or hydronium carbamate ions are thought to bind through one ethylamine (Figure 5a).[69] Note that ammonium carbamates can be present in both dry and humid conditions; they are also the only species illustrated in Figure 5a that results in interchain ionic cross-linking.

As the fluorescence and NMR experiments clearly suggest that humidity increases polymer mobility, we first verified whether ammonium carbamates were formed in significant concentrations in PEI:Al_2O_3 when flowing humid CO_2. To this end, we performed DRIFTS on pre-humidified PEI:Al_2O_3 following the same protocol as for the fluorescence measurements, flowing 400 ppm CO_2 at 0, 11, 33, 53, 75, and 100% RH for 90 min. The background for each sample was collected just before exposing the sample to the humidified CO_2 stream. From the spectra shown in Figure 5b,c, we can ascertain that the surface reactions between CO_2 and PEI:Al_2O_3 vary with

https://doi.org/10.1021/acs.jpcc.3c03653
J. Phys. Chem. C 2023, 127, 15363−15374

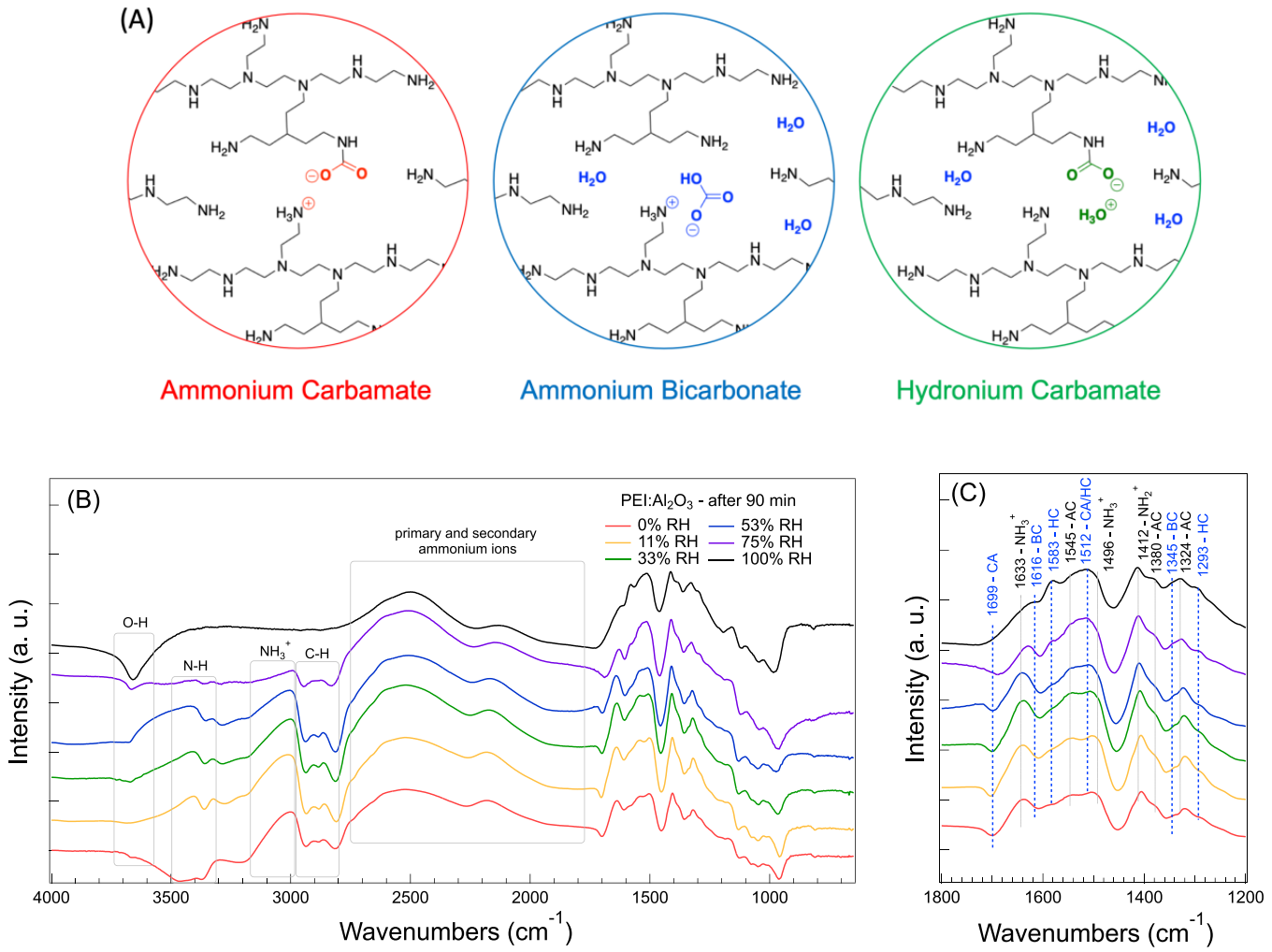

Figure 5. (Top, a) Possible molecular structures resulting from CO_2 capture by PEI in dry (red) and humid conditions (red, blue, and green). (Bottom) DRIFT spectra of PEI:Al_2O_3 after 90 min of exposure to 400 ppm CO_2 at 0, 11, 33, 53, 75, and 100% RH. The spectra are offset for clarity. A new sample was used for each RH condition. (b) Significant bands and peaks are assigned in the range of 4000−1800 cm^{-1}. (c) Peaks of interest are assigned between 1800 and 1200 cm^{-1}, where the peaks increasing as a function of increasing humidity are depicted in dashed blue lines, and the other features are highlighted with solid gray lines. The peak assignment of panel (b) is recorded in Table S1 and panel (c) in Table 2. CA refers to carbamic acid, BC to bicarbonate, AC to ammonium carbamate, and HC to hydronium carbamate.

RH. Under dry conditions, the band associated with primary amines in PEI at 3305−3602 cm^{-1} is depleted as they are the main binding sites for CO_2. In contrast, hydroxyl groups (−OH at 3656 cm^{-1}) play an increasing role in the mechanism for 75−100% RH CO_2 streams. Furthermore, as a function of increasing humidity, characteristic bands associated with $-CH_2$ and $-CH_3$ in PEI (at 2792−2966 cm^{-1}) are less depleted, and the peaks associated with ammonium carbamates ($-NH_3^+/-NH_2^+$) spanning from 1800 to 2790 cm^{-1} are less intense. This is especially visible in the time-dependent spectra shown in Figure S7 in the SI, where these features were almost absent after 5 min at 100% RH.

Many species of interest have absorption peaks in the region between 1800 and 1200 cm^{-1}, which makes it challenging to assign peaks properly, sometimes leading to disputes in the community.[73] Furthermore, PEI:Al_2O_3 is a highly heterogeneous system, with primary, secondary, and tertiary amines present in PEI and a large pore size distribution in Al_2O_3. As such, this composite system is rarely chosen for systematic studies of the role of humidity using DRIFTS. Based on the combined literature from multiple aminopolymers, small-molecule amines, and mostly silica-based supports, we propose the tentative peak assignments in Table 2, where the peaks increasing with humidity are listed in bold.

IR signatures from ammonium carbamate can be observed for all levels of humidity, while other peaks grew or appeared only as humid CO_2 was introduced to the system. Such peaks have been assigned to carbamic acid at 1699 and 1512 cm^{-1}, some weak contributions of bicarbonate at 1345 and 1616 cm^{-1} were observed, and the features at 1293 and 1582 cm^{-1} best fit the absorption of hydronium carbamate, which has been mainly reported for tetraethylenepentamine (TEPA) thin films by Miller and co-workers.[70] The authors also computationally validated the rapid diffusion of CO_2 through hydronium carbamate species in TEPA during humid conditions. While the formation of bicarbonates in humid conditions is sometimes put forward as the major mechanism,[59] we measure only subtle contributions from these species, which is in line with the measurement of bicarbonate formation predominantly with tertiary amines[57] or with secondary amines at low PEI loadings.[58] In the study of our materials under humid conditions, peaks associated with

https://doi.org/10.1021/acs.jpcc.3c03653
J. Phys. Chem. C 2023, 127, 15363−15374

Table 2. Assignment of IR Peaks/Bands Observed in Humidified PEI/Al_2O_3 Composites

wavenumber (cm^{-1})	assignment	species	references
1293[a,b]	**$N_{(1)}$-CO_2**	**hydronium carbamate**	70
1324	$NCOO^-$ skeletal vibration	ammonium carbamate	58, 71, 74
1345	**C-O sym stretch**	**bicarbonate**	57, 58
1380	COO^- sym stretch	ammonium carbamate	58, 60, 73
1412	NH_2^+ deformation	NH_2^+	75
1496	NH_3^+ sym deformation	NH_3^+	58, 75, 76
1512	**CN stretch, COO^- asym stretch**	**carbamic acid, hydronium carbamate**	76, 70
1545	COO^- stretch	ammonium carbamate	71, 76
1583	**COO^- asym stretch**	**hydronium carbamate**	70
1616	**C-O asym stretch**	**bicarbonate**	57
1633	NH_3^+ asym deformation	NH_3^+	58, 71, 73, 75, 76
1699	C=O stretch	carbamic acid	58, 60, 71, 75, 76

[a]Peaks that increase with RH are listed in bold. [b]Some peak positions shift with humidity. Peak positions are reported for the 100% RH sample.

carbamic acid and hydronium carbamate experience the highest increase in intensity. Unlike in ammonium carbamates, captured CO_2 in the form of carbamic acid and hydronium carbamate does not promote interchain ionic cross-linking that results in decreased polymer mobility. The results provide quantitative support at the molecular level for understanding humidity-promoted polymer mobility that is inferred by the fluorescence and NMR relaxometry measurements.

Finally, we note that Potter and co-workers demonstrated that the acidity of Al_2O_3 supports can impact the reaction mechanism of CO_2 with tethered aminopropylsilyl groups in dry conditions.[60] Especially at low amine loading, CO_2 was shown to interact directly with the Al_2O_3 support, while these interactions were suppressed at higher amine loadings. We did perform both small- and wide-angle X-ray scattering (SAXS and WAXS) measurements to probe the role of Al_2O_3 in our system (Figure S8). While we observed that the impact of CO_2 on the Al_2O_3 crystal structure is negligible at 100% RH conditions, likely due to the high levels of hydroxylation on the surface of Al_2O_3, in dry conditions, the presence of CO_2 dramatically degrades the Al_2O_3 crystal structure (see brief discussion in the SI). The result serves to highlight the non-innocent role that the changing support may have on influencing PEI mobility at the polymer−support interface as the composite uptakes CO_2. However, a more detailed study of the nature of the degradation of the Al_2O_3 crystal structure as a function of CO_2 capture is outside the scope of this current manuscript and will be reported elsewhere.

CONCLUSIONS

This work demonstrated the value of two benchtop techniques for studying polymer mobility within nanocomposite DAC materials as a function of CO_2 and water adsorption. First, we assessed the efficacy of employing a fluorescent probe technique for understanding polymer mobility in a series of humidified PEI:Al_2O_3 composites, correlating measurements of moisture uptake with changes in the emission spectra. We then did the same for CO_2 sorption in these materials across a range of temperatures as well as values of RH. We correlated the fluorescence data and implied changes in mobility with data from a second benchtop technique, namely, a portable magnetic resonance sensor known as the NMR MOUSE. Changes in spin−spin and spin−lattice relaxation measurements with this technique helped corroborate conclusions drawn from fluorescence regarding polymer mobility. We then coupled all this information with DRIFTS data, which provided molecular level support for understanding the fundamental underpinnings of humidity-promoted polymer mobility in these materials observed with both fluorescence and NMR relaxometry measurements. Given the large matrix of variables that can influence polymer mobility in confinement, which continue to change as a function of sorbent lifetime and cycling, these high-throughput techniques for quantifying *in operando* changes in mobility position the field for rapid advancement in understanding and deployment of these materials in real-world DAC systems.

ASSOCIATED CONTENT

Supporting Information

The Supporting Information is available free of charge at https://pubs.acs.org/doi/10.1021/acs.jpcc.3c03653.

Emission spectra, DRIFTS data, NMR relaxometry data, CO_2 cycling experiment, SAXS/WAXS data, and discussion (PDF)

AUTHOR INFORMATION

Corresponding Author

Wade A. Braunecker − *Department of Chemistry, Colorado School of Mines, Golden, Colorado 80401, United States; National Renewable Energy Laboratory, Golden, Colorado 80401, United States;* orcid.org/0000-0003-0773-9580; Email: Wade.Braunecker@nrel.gov

Authors

Glory A. Russell-Parks − *Department of Chemistry, Colorado School of Mines, Golden, Colorado 80401, United States; National Renewable Energy Laboratory, Golden, Colorado 80401, United States;* orcid.org/0000-0001-9059-1681

Noemi Leick − *National Renewable Energy Laboratory, Golden, Colorado 80401, United States;* orcid.org/0000-0002-2014-6264

Maxwell A. T. Marple − *Lawrence Livermore National Laboratory, Livermore, California 94550, United States;* orcid.org/0000-0001-5251-8301

Nicholas A. Strange − *Stanford Synchrotron Radiation Lightsource, SLAC National Accelerator Laboratory, Menlo Park, California 94025, United States;* orcid.org/0000-0001-5699-7274

Brian G. Trewyn − *Department of Chemistry and Materials Science Program, Colorado School of Mines, Golden, Colorado 80401, United States; National Renewable Energy Laboratory, Golden, Colorado 80401, United States;* orcid.org/0000-0003-4027-7402

Simon H. Pang − *Lawrence Livermore National Laboratory, Livermore, California 94550, United States;* orcid.org/0000-0003-2913-1648

Complete contact information is available at: https://pubs.acs.org/10.1021/acs.jpcc.3c03653

https://doi.org/10.1021/acs.jpcc.3c03653
J. Phys. Chem. C 2023, 127, 15363−15374

Notes

The authors declare no competing financial interest.

■ ACKNOWLEDGMENTS

This work was authored in part by Alliance for Sustainable Energy, LLC, the manager and operator of the National Renewable Energy Laboratory for the U.S. Department of Energy (DOE) under contract no. DE-AC36-08GO28308. Work at Lawrence Livermore National Laboratory was performed under the auspices of the U.S. DOE under contract DE-AC52-07NA27344. Use of the Stanford Synchrotron Radiation Lightsource, SLAC National Accelerator Laboratory, is supported by the U.S. DOE, Office of Science, Office of Basic Energy Sciences under contract no. DE-AC02-76SF00515. This work was supported by the U.S. DOE, Office of Science, Basic Energy Sciences, Materials Sciences and Engineering Division in response to the DOE National Laboratory Announcement Number LAB 20-2303: Materials and Chemical Sciences Research for Direct Air Capture of Carbon Dioxide. The views expressed in the article do not necessarily represent the views of the DOE or the U.S. Government. The U.S. Government retains and the publisher, by accepting the article for publication, acknowledges that the U.S. Government retains a nonexclusive, paid-up, irrevocable, worldwide license to publish or reproduce the published form of this work, or allow others to do so, for U.S. Government purposes.

■ REFERENCES

(1) Boul, P. J., *Energy Transition: Climate Action and Circularity*. American Chemical Society: Washington, DC, 2022; Vol. *1412*.

(2) *The challenge of decarbonizing heavy industry*. https://www.brookings.edu/research/the-challenge-of-decarbonizing-heavy-industry/, accessed July 2023.

(3) Gabrielli, P.; Gazzani, M.; Mazzotti, M. The Role of Carbon Capture and Utilization, Carbon Capture and Storage, and Biomass to Enable a Net-Zero-CO2 Emissions Chemical Industry. *Ind. Eng. Chem. Res.* **2020**, *59*, 7033−7045.

(4) Beuttler, C.; Charles, L.; Wurzbacher, J. The Role of Direct Air Capture in Mitigation of Anthropogenic Greenhouse Gas Emissions. *Front. Clim.* **2019**, *1*, 1−7.

(5) Shi, X.; Xiao, H.; Azarabadi, H.; Song, J.; Wu, X.; Chen, X.; Lackner, K. S. Sorbents for the Direct Capture of CO2 from Ambient Air. *Angew. Chem., Int. Ed.* **2020**, *59*, 6984−7006.

(6) McQueen, N.; Gomes, K. V.; McCormick, C.; Blumanthal, K.; Pisciotta, M.; Wilcox, J. A review of direct air capture (DAC): scaling up commercial technologies and innovating for the future. *Prog. Energy* **2021**, *3*, No. 032001.

(7) *Global Thermostat unveils one of the world's largest units for removing carbon dioxide directly from the air*. https://www.globalthermostat.com/news-and-updates/global-thermostat-colorado-headquarters, accessed July 2023.

(8) Goeppert, A.; Czaun, M.; May, R. B.; Prakash, G. K. S.; Olah, G. A.; Narayanan, S. R. Carbon Dioxide Capture from the Air Using a Polyamine Based Regenerable Solid Adsorbent. *J. Am. Chem. Soc.* **2011**, *133*, 20164−20167.

(9) Chaikittisilp, W.; Kim, H.-J.; Jones, C. W. Mesoporous Alumina-Supported Amines as Potential Steam-Stable Adsorbents for Capturing CO2 from Simulated Flue Gas and Ambient Air. *Energy Fuels* **2011**, *25*, 5528−5537.

(10) Sakwa-Novak, M. A.; Jones, C. W. Steam Induced Structural Changes of a Poly(ethylenimine) Impregnated γ-Alumina Sorbent for CO2 Extraction from Ambient Air. *ACS Appl. Mater. Interfaces* **2014**, *6*, 9245−9255.

(11) Zhang, H.; Goeppert, A.; Prakash, G. K. S.; Olah, G. Applicability of linear polyethylenimine supported on nano-silica for the adsorption of CO2 from various sources including dry air. *RSC Adv.* **2015**, *5*, 52550−52562.

(12) Sakwa-Novak, M. A.; Yoo, C.-J.; Tan, S.; Rashidi, F.; Jones, C. W. Poly(ethylenimine)-Functionalized Monolithic Alumina Honeycomb Adsorbents for CO2 Capture from Air. *ChemSusChem* **2016**, *9*, 1859−1868.

(13) Kwon, H. T.; Sakwa-Novak, M. A.; Pang, S. H.; Sujan, A. R.; Ping, E. W.; Jones, C. W. Aminopolymer-Impregnated Hierarchical Silica Structures: Unexpected Equivalent CO2 Uptake under Simulated Air Capture and Flue Gas Capture Conditions. *Chem. Mater.* **2019**, *31*, 5229−5237.

(14) Sujan, A. R.; Pang, S. H.; Zhu, G.; Jones, C. W.; Lively, R. P. Direct CO2 Capture from Air using Poly(ethylenimine)-Loaded Polymer/Silica Fiber Sorbents. *ACS Sustainable Chem. Eng.* **2019**, *7*, 5264−5273.

(15) Rosu, C.; Pang, S. H.; Sujan, A. R.; Sakwa-Novak, M. A.; Ping, E. W.; Jones, C. W. Effect of Extended Aging and Oxidation on Linear Poly(propylenimine)-Mesoporous Silica Composites for CO2 Capture from Simulated Air and Flue Gas Streams. *ACS Appl. Mater. Interfaces* **2020**, *12*, 38085−38097.

(16) Racicot, J.; Li, S.; Clabaugh, A.; Hertz, C.; Akhade, S. A.; Ping, E. W.; Pang, S. H.; Sakwa-Novak, M. A. Volatile Products of the Autoxidation of Poly(ethylenimine) in CO2 Sorbents. *J. Phys. Chem. C* **2022**, *126*, 8807−8816.

(17) Li, S.; Cerón, M. R.; Eshelman, H. V.; Varni, A. J.; Maiti, A.; Akhade, S.; Pang, S. H. Probing the Kinetic Origin of Varying Oxidative Stability of Ethyl- vs. Propyl-spaced Amines for Direct Air Capture. *ChemSusChem* **2023**, *16*, No. e202201908.

(18) Rim, G.; Kong, F.; Song, M.; Rosu, C.; Priyadarshini, P.; Lively, R. P.; Jones, C. W. Sub-Ambient Temperature Direct Air Capture of CO2 using Amine-Impregnated MIL-101(Cr) Enables Ambient Temperature CO2 Recovery. *JACS Au* **2022**, *2*, 380−393.

(19) Miao, Y.; Wang, Y.; Ge, B.; He, Z.; Zhu, X.; Li, J.; Liu, S.; Yu, L. Mixed Diethanolamine and Polyethyleneimine with Enhanced CO2 Capture Capacity from Air. *Adv. Sci.* **2023**, *10*, 2207253.

(20) Kong, F.; Rim, G.; Song, M.; Rosu, C.; Priyadarshini, P.; Lively, R. P.; Realff, M. J.; Jones, C. W. Research needs targeting direct air capture of carbon dioxide: Material & process performance characteristics under realistic environmental conditions. *Korean J. Chem. Eng.* **2022**, *39*, 1−19.

(21) Moon, H. J.; Carrillo, J.-M.; Leisen, J.; Sumpter, B. G.; Osti, N. C.; Tyagi, M.; Jones, C. W. Understanding the Impacts of Support−Polymer Interactions on the Dynamics of Poly(ethyleneimine) Confined in Mesoporous SBA-15. *J. Am. Chem. Soc.* **2022**, *144*, 11664−11675.

(22) Robeson, L. M.; Liu, Q.; Freeman, B. D.; Paul, D. R. Comparison of transport properties of rubbery and glassy polymers and the relevance to the upper bound relationship. *J. Membr. Sci.* **2015**, *476*, 421−431.

(23) Sakwa-Novak, M. A.; Tan, S.; Jones, C. W. Role of Additives in Composite PEI/Oxide CO2 Adsorbents: Enhancement in the Amine Efficiency of Supported PEI by PEG in CO2 Capture from Simulated Ambient Air. *ACS Appl. Mater. Interfaces* **2015**, *7*, 24748−24759.

(24) Carneiro, J. S. A.; Innocenti, G.; Moon, H. J.; Guta, Y.; Proaño, L.; Sievers, C.; Sakwa-Novak, M. A.; Ping, E. W.; Jones, C. W. Insights into the Oxidative Degradation Mechanism of Solid Amine Sorbents for CO2 Capture from Air: Roles of Atmospheric Water. *Angew. Chem., Int. Ed.* **2023**, *135*, No. e202302887.

(25) Garcia, S. J. Effect of polymer architecture on the intrinsic self-healing character of polymers. *E. Polym. J.* **2014**, *53*, 118−125.

(26) Paeng, K.; Richert, R.; Ediger, M. D. Molecular mobility in supported thin films of polystyrene, poly(methyl methacrylate), and poly(2-vinyl pyridine) probed by dye reorientation. *Soft Matter* **2012**, *8*, 819−826.

(27) Priestley, R. D.; Ellison, C. J.; Broadbelt, L. J.; Torkelson, J. M. Structural Relaxation of Polymer Glasses at Surfaces, Interfaces, and In Between. *Science* **2005**, *309*, 456−459.

(28) Baglay, R. R.; Roth, C. B.; et al. *J. Chem. Phys.* **2017**, *146*, 203307.

(29) Said, R. B.; Kolle, J. M.; Essalah, K.; Tangour, B.; Sayari, A. A Unified Approach to CO2−Amine Reaction Mechanisms. *ACS Omega* **2020**, *5*, 26125−26133.
(30) Jahandar Lashaki, M.; Khiavi, S.; Sayari, A. Stability of amine-functionalized CO2 adsorbents: a multifaceted puzzle. *Chem. Soc. Rev.* **2019**, *48*, 3320−3405.
(31) Sayari, A.; Heydari-Gorji, A.; Yang, Y. CO2-Induced Degradation of Amine-Containing Adsorbents: Reaction Products and Pathways. *J. Am. Chem. Soc.* **2012**, *134*, 13834−13842.
(32) Ellison, C. J.; Torkelson, J. M. The distribution of glass-transition temperatures in nanoscopically confined glass formers. *Nat. Mater.* **2003**, *2*, 695−700.
(33) Elmahdy, M. M.; Chrissopoulou, K.; Afratis, A.; Floudas, G.; Anastasiadis, S. H. Effect of Confinement on Polymer Segmental Motion and Ion Mobility in PEO/Layered Silicate Nanocomposites. *Macromolecules* **2006**, *39*, 5170−5173.
(34) Uemura, T.; Yanai, N.; Watanabe, S.; Tanaka, H.; Numaguchi, R.; Miyahara, M. T.; Ohta, Y.; Nagaoka, M.; Kitagawa, S. Unveiling thermal transitions of polymers in subnanometre pores. *Nat. Commun.* **2010**, *1*, 83.
(35) Correll, H.; Leick, N.; Mow, R. E.; Russell-Parks, G. A.; Pang, S. H.; Gennett, T.; Braunecker, W. A. Fluorescent Probe of Amino-polymer Mobility in Bulk and in Nanoconfined Direct Air CO2 Capture Supports. *J. Phys. Chem. C* **2022**, *126*, 10419−10428.
(36) Efremov, M. Y.; Warren, J. T.; Olson, E. A.; Zhang, M.; Kwan, A. T.; Allen, L. H. Thin-Film Differential Scanning Calorimetry: A New Probe for Assignment of the Glass Transition of Ultrathin Polymer Films. *Macromolecules* **2002**, *35*, 1481−1483.
(37) Mapesa, E. U.; Cantillo, N. M.; Hamilton, S. T.; Harris, M. A.; Zawodzinski, T. A., Jr.; Alissa Park, A.-H.; Sangoro, J. Localized and Collective Dynamics in Liquid-like Polyethylenimine-Based Nanoparticle Organic Hybrid Materials. *Macromolecules* **2021**, *54*, 2296−2305.
(38) Holewinski, A.; Sakwa-Novak, M. A.; Jones, C. W. Linking CO2 Sorption Performance to Polymer Morphology in Amino-polymer/Silica Composites through Neutron Scattering. *J. Am. Chem. Soc.* **2015**, *137*, 11749−11759.
(39) Holewinski, A.; Sakwa-Novak, M. A.; Carrillo, J.-M. Y.; Potter, M. E.; Ellebracht, N.; Rother, G.; Sumpter, B. G.; Jones, C. W. Aminopolymer Mobility and Support Interactions in Silica-PEI Composites for CO2 Capture Applications: A Quasielastic Neutron Scattering Study. *J. Phys. Chem. B* **2017**, *121*, 6721−6731.
(40) Stafford, C. M.; Harrison, C.; Beers, K. L.; Karim, A.; Amis, E. J.; VanLandingham, M. R.; Kim, H.-C.; Volksen, W.; Miller, R. D.; Simonyi, E. E. A buckling-based metrology for measuring the elastic moduli of polymeric thin films. *Nat. Mater.* **2004**, *3*, 545−550.
(41) O'Connell, P. A.; McKenna, G. B. The stiffening of ultrathin polymer films in the rubbery regime: The relative contributions of membrane stress and surface tension. *J. Polym. Sci., Part B: Polym. Phys.* **2009**, *47*, 2441−2448.
(42) Ellison, C. J.; Kim, S. D.; Hall, D. B.; Torkelson, J. M. Confinement and processing effects on glass transition temperature and physical aging in ultrathin polymer films: Novel fluorescence measurements. *Eur. Phys. J. E: Soft Matter Biol. Phys.* **2002**, *8*, 155−166.
(43) Mundra, M. K.; Ellison, C. J.; Rittigstein, P.; Torkelson, J. M. Fluorescence studies of confinement in polymer films and nanocomposites: Glass transition temperature, plasticizer effects, and sensitivity to stress relaxation and local polarity. *Eur. Phys. J. Spec. Top.* **2007**, *141*, 143.
(44) Askar, S.; Torkelson, J. M. Stiffness of thin, supported polystyrene films: Free-surface, substrate, and confinement effects characterized via self-referencing fluorescence. *Polymer* **2016**, *99*, 417−426.
(45) Burroughs, M. J.; Christie, D.; Gray, L. A. G.; Chowdhury, M.; Priestley, R. D. 21st Century Advances in Fluorescence Techniques to Characterize Glass-Forming Polymers at the Nanoscale. *Macromol. Chem. Phys.* **2018**, *219*, 1700368.
(46) Eidmann, G.; Savelsberg, R.; Blümler, P.; Blümich, B. The NMR MOUSE, a Mobile Universal Surface Explorer. *J. Magn. Reson., Ser. A* **1996**, *122*, 104−109.
(47) Potter, M. E.; Pang, S. H.; Jones, C. W. Adsorption Microcalorimetry of CO2 in Confined Aminopolymers. *Langmuir* **2017**, *33*, 117−124.
(48) Barbara, P. F.; Rand, S. D.; Rentzepis, P. M. Direct measurements of tetraphenylethylene torsional motion by picosecond spectroscopy. *J. Am. Chem. Soc.* **1981**, *103*, 2156−2162.
(49) Mei, J.; Leung, N. L. C.; Kwok, R. T. K.; Lam, J. W. Y.; Tang, B. Z. Aggregation-Induced Emission: Together We Shine, United We Soar! *Chem. Rev.* **2015**, *115*, 11718−11940.
(50) Gao, Y.-J.; Chang, X.-P.; Liu, X.-Y.; Li, Q.-S.; Cui, G.; Thiel, W. Excited-State Decay Paths in Tetraphenylethene Derivatives. *J. Phys. Chem. A* **2017**, *121*, 2572−2579.
(51) Kayal, S.; Roy, K.; Umapathy, S. Femtosecond coherent nuclear dynamics of excited tetraphenylethylene: Ultrafast transient absorption and ultrafast Raman loss spectroscopic studies. *J. Chem. Phys.* **2018**, *148*, 1−10.
(52) Hughes, B. K.; Braunecker, W. A.; Ferguson, A. J.; Kemper, T. W.; Larsen, R. E.; Gennett, T. Quenching of the Perylene Fluorophore by Stable Nitroxide Radical-Containing Macromolecules. *J. Phys. Chem. B* **2014**, *118*, 12541−12548.
(53) Maillard, J.; Klehs, K.; Rumble, C.; Vauthey, E.; Heilemann, M.; Fürstenberg, A. Universal quenching of common fluorescent probes by water and alcohols. *Chem. Sci.* **2021**, *12*, 1352−1362.
(54) Li, S.; Andrade, M. F. C.; Varni, A. J.; Russell-Parks, G. A.; Braunecker, W. A.; Hunters-Sellars, E.; Marple, M. A. T.; Pang, S. H. Enhanced Hydrogen Bonding via Epoxide-functionalization Restricts Mobility in Poly(ethylenimine) for CO2 Capture. *ChemRxiv* **2023**, DOI: 10.26434/chemrxiv-2023-l5j08.
(55) Zhang, J.; Corpstein, C. D.; Li, T. Intracellular uptake of nanocrystals: Probing with aggregation-induced emission of fluorescence and kinetic modeling. *Acta Pharm. Sin. B* **2021**, *11*, 1021−1029.
(56) Ali, A.; Striolo, A.; Cole, D. R. CO2 Solubility in Aqueous Electrolyte Solutions Confined in Calcite Nanopores. *J. Phys. Chem. C* **2021**, *125*, 12333−12341.
(57) Lee, J. J.; Chen, C.-H.; Shimon, D.; Hayes, S. E.; Sievers, C.; Jones, C. W. Effect of Humidity on the CO2 Adsorption of Tertiary Amine Grafted SBA-15. *J. Phys. Chem. C* **2017**, *121*, 23480−23487.
(58) Didas, S. A.; Sakwa-Novak, M. A.; Foo, G. S.; Sievers, C.; Jones, C. W. Effect of Amine Surface Coverage on the Co-Adsorption of CO2 and Water: Spectral Deconvolution of Adsorbed Species. *J. Phys. Chem. Lett.* **2014**, *5*, 4194−4200.
(59) Hack, J.; Maeda, N.; Meier, D. M. Review on CO2 Capture Using Amine-Functionalized Materials. *ACS Omega* **2022**, *7*, 39520−39530.
(60) Potter, M. E.; Cho, K. M.; Lee, J. J.; Jones, C. W. Role of Alumina Basicity in CO2 Uptake in 3-Aminopropylsilyl-Grafted Alumina Adsorbents. *ChemSusChem* **2017**, *10*, 2192−2201.
(61) Kumar, R.; Bandyopadhyay, M.; Pandey, M.; Tsunoji, N. Amine-impregnated nanoarchitectonics of mesoporous silica for capturing dry and humid 400 ppm carbon dioxide: A comparative study. *Microporous Mesoporous Mater.* **2022**, *338*, No. 111956.
(62) Casanova, F.; Perlo, J.; Blümich, B. Single-Sided NMR. In *Single-Sided NMR*, Casanova, F.; Perlo, J.; Blümich, B., Eds. Springer Berlin Heidelberg: Berlin, Heidelberg, 2011; pp. 1−10.
(63) Blümich, B.; Perlo, J.; Casanova, F. Mobile single-sided NMR. *Prog. Nucl. Magn. Reson. Spectrosc.* **2008**, *52*, 197−269.
(64) Levitt, M. H. *Spin Dynamics: Basics of Nuclear Magnetic Resonance;* 2nd Ed. John Wiley & Sons: Hoboken, New Jersey, 2013.
(65) Whittaker, A. K. NMR Studies of Cross linked Polymers. In *Annual Reports on NMR Spectroscopy*; Webb, G. A.; Ando, I., Eds. Academic Press: 1997; Vol. *34*, pp. 105−183, DOI: 10.1016/S0066-4103(08)60102-7.
(66) Wiesner, B.; Kohn, B.; Mende, M.; Scheler, U. Polymer Chain Mobility under Shear—A Rheo-NMR Investigation. *Polymer* **2018**, *10*, 1231.

(67) Zhan, P.; Zhang, W.; Jacobs, I. E.; Nisson, D. M.; Xie, R.; Weissen, A. R.; Colby, R. H.; Moulé, A. J.; Milner, S. T.; Maranas, J. K.; Gomez, E. D.; et al. Side chain length affects backbone dynamics in poly(3-alkylthiophene)s. *J. Polym. Sci., Part B: Polym. Phys.* **2018**, *56*, 1193−1202.
(68) Pietrasik, J.; Sumerlin, B. S.; Lee, H.-I.; Gil, R. R.; Matyjaszewski, K. Structural mobility of molecular bottle-brushes investigated by NMR relaxation dynamics. *Polymer* **2007**, *48*, 496−501.
(69) Li, K.; Kress, J. D.; Mebane, D. S. The Mechanism of CO2 Adsorption under Dry and Humid Conditions in Mesoporous Silica-Supported Amine Sorbents. *J. Phys. Chem. C* **2016**, *120*, 23683−23691.
(70) Miller, D. D.; Yu, J.; Chuang, S. S. C. Unraveling the Structure and Binding Energy of Adsorbed CO2/H2O on Amine Sorbents. *J. Phys. Chem. C* **2020**, *124*, 24677−24689.
(71) Wilfong, W. C.; Srikanth, C. S.; Chuang, S. S. C. In Situ ATR and DRIFTS Studies of the Nature of Adsorbed CO2 on Tetraethylenepentamine Films. *ACS Appl. Mater. Interfaces* **2014**, *6*, 13617−13626.
(72) Kim, H.-J.; Chaikittisilp, W.; Jang, K.-S.; Didas, S. A.; Johnson, J. R.; Koros, W. J.; Nair, S.; Jones, C. W. Aziridine-Functionalized Mesoporous Silica Membranes on Polymeric Hollow Fibers: Synthesis and Single-Component CO2 and N2 Permeation Properties. *Ind. Eng. Chem. Res.* **2015**, *54*, 4407−4413.
(73) Bacsik, Z.; Hedin, N. Effects of carbon dioxide captured from ambient air on the infrared spectra of supported amines. *Vib. Spectrosc.* **2016**, *87*, 215−221.
(74) Sun, C.; Dutta, P. K. Infrared Spectroscopic Study of Reaction of Carbon Dioxide with Aqueous Monoethanolamine Solutions. *Ind. Eng. Chem. Res.* **2016**, *55*, 6276−6283.
(75) Zhai, Y.; Chuang, S. S. C. Enhancing Degradation Resistance of Polyethylenimine for CO2 Capture with Cross-Linked Poly(vinyl alcohol). *Ind. Eng. Chem. Res.* **2017**, *56*, 13766−13775.
(76) Hedin, N.; Bacsik, Z. Perspectives on the adsorption of CO2 on amine-modified silica studied by infrared spectroscopy. *Curr. Opin. Green Sustainable Chem.* **2019**, *16*, 13−19.

https://doi.org/10.1021/acs.jpcc.3c03653
J. Phys. Chem. C 2023, 127, 15363−15374